

Fragmentation of 2,5-diketopiperazine cyclic dipeptide ions

© A.A. BasalaeV,¹ V.V. Kuz'michev,¹ M.N. Panov,¹ A.V. Petrov,² O.V. Smirnov¹

¹ Ioffe Institute, St. Petersburg, Russia

² Saint Petersburg State University, Institute of Chemistry, St. Petersburg, Russia

e-mail: a.basalaeV@mail.ioffe.ru

Received December 6, 2021

Revised December 6, 2021

Accepted March 3, 2022

The mechanism of radiation damage to 2,5-diketopiperazine (DKP, C₄H₆N₂O₂) molecules in the gas phase upon interaction with He²⁺ ions with an energy E_p = 4 keV/u has been investigated. The relative cross sections of various elementary processes occurring in single collisions of DKP with ions have been measured for the first time. The channels of fragmentation processes of singly charged ions have been studied experimentally. The DFT method was used to calculate the geometry of molecules and singly charged DKP ions, as well as the energies of the main experimentally observed channels of fragmentation of these ions.

Keywords: electron capture, dipeptides, molecular ion fragmentation.

DOI: 10.21883/TP.2022.07.54477.309-21

Introduction

Peptides — are biological molecules formed by chains of amino acid residues with peptide bond formed by connection of end amine group of one amino acid with end carboxyl group of the other one. Impact of ionizing radiation on peptides, in addition to polypeptide chain break, may change amino acid composition due to separation of side chain fragments of amino acid residue chains in peptide ionization [1]. Such structural damages may cause loss of functional activity of peptide.

Radiation resistance of peptides may be studied by mass-spectrometer analysis of molecular ion fragmentation formed in single-time molecular collision process in gas environment with ionising particle. Such approach allows to avoid radiation and chemical process flowing during the study of interaction between ionising radiation and solutions or solid body [2].

Dipeptide molecules composed of two amino acid residues are simple peptides. Cyclic dipeptides which often occur in nature are formed due to formation of one more peptide bond in linear dipeptide. All them are derivatives of 2,5-diketopiperazine (DKP) or cyclo(Gly-Gly).

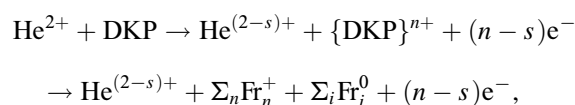
Dipeptide molecule ionization are rarely studied. For some of them, mass-spectra fragments formed by electron impact ionization are studied [3]. In [4], mass spectra formed by electron impact ionization of 22 dipeptides, several deuterated dipeptides and two cyclic DKP dipeptides and cyclo(Ala-Ala) were studied.

Photoelectron spectroscopy method was used to carry out experimental research of electron structure of dipeptides in gas phase such as Gly-Gly [5] and DKP, cyclo(Leu-Pro), and cyclo(Phe-Pro) [6], and also more complex cyclic dipeptides containing six-membered DKP ring [7]. Experimentally obtained spectra of valent and core levels are interpreted herein using *ab initio* calculations. Studies

of structural characteristics of cyclic dipeptide molecules were studied in [8,9]. In [8], energy characteristics of cyclization reactions of linear dipeptides were calculated and cyclization reaction activation energies were defined. They also detected that most of cyclization reactions are exothermic reactions. In [10], structural characteristics of isolated molecule cyclo(Gly-Leu) were calculated.

It should be noted that the study of isolated peptide molecules is hindered by possible molecule decomposition by heating [11,12]. [4] showed that mass spectra formed by electron impact ionization for linear dipeptides often represent summarized dipeptide and cyclopeptide spectra formed in the initial dipeptide sublimation process.

The purpose of this research was to study radiation damage of isolated DKP molecules by measurement of relative cross-sections of various elementary processes which occur when charge state of collision partners changes:



where $\{\text{DKP}\}^{n+}$ — intermediate state of molecular ion formed during He²⁺ ion trapping of *s*-electrons (*s* = 1, 2), (*n*−*s*) — number of free electrons occurring during trapping, Fr_{*n*}⁺ — fragment ions are generally single-charged, Fr_{*i*}⁰ — neutral fragments. Charge states of interacting particles are described by three numbers $\{2(2-s)n\}$. Relative cross-sections of corresponding processes are designated as $\sigma_n^{2(2-s)}$.

To study fragmentation of single-charged molecular ions DKP⁺, quantum chemical calculations were carried out. Fragmentation channels of single-charged molecular ions were chosen for the analysis according to the experimental mass spectra of fragment ions Fr_{*n*}⁺ formed during trapping of one electron {211} by ions He²⁺.

1. Experimental procedure

The research was carried out using experimental procedure earlier used to study interaction between ions and amino acids and nucleic acid bases [13,14]. The interaction region of monokinetic well collimated ion beam ${}^3\text{He}^{2+}$ with energy 4 keV/u (velocity $V_p = 0.41$ a.u.) with effusion jet of target molecules was in 150 V/cm homogenous electric field which pulled out the formed target ions into ion optical system of linear time-of-flight mass spectrometer. After optical system of the mass-spectrometer, ions were additionally accelerated by 14 kV voltage to enable their recording with high and almost the same efficiency irrespective of mass, in computation mode.

Charge condition of charges after the interaction was defined by electrostatic analyzer. The arrival time of He^+ ions or He atoms, formed after trapping of one or two electrons, to the detector served as a start signal of the recording system. time-of-flight mass spectrometer detector signals were recorded in „multistop“ mode. Ion optical system of the mass-spectrometer ensured full collection of ion fragments with initial energies up to 9 eV.

effusion molecule jet isolated by a mechanical valve for background measurement was achieved by furnace heating of crystalline DKP. Capillary forming the molecular jet and container with the test substance were made from PTFE which allowed to avoid the impact of catalytic action of the furnace material on the test substance sublimation. Absolute furnace temperature was measured with accuracy $\pm 0.12\%$, and its temperature drift during spectra measurement did not exceed 0.4°C . During the test, sample heating temperatures were selected to ensure single-time collision mode in the interaction region of the effusion jet with input particles.

Relative cross-sections of charge state changes of collision partners were determined according to mass spectra analysis without background component. Mass spectra obtained after background subtraction were rated for the amount of substance that has flown through the interaction region and incident ion beam current integral. For measurements processing, mass spectra were formed for the processes with simultaneous forming of one, two, three or four charged molecular fragments. Thus, single-electron trapping {211} (with formation of one charged fragment), electron trapping with ionization {212} (two charged fragments were formed) and electron trapping with double ionization {213} (with formation of three charged fragments) processes were separated. Also process caused by trapping of two electron were separated. Two-electron trapping {202} (two charged fragments were formed), trapping of two electron with ionization {203} (three charged fragments were formed) and trapping of two electrons with double ionization {204} (four charged fragments were formed). Typical mass spectra of molecular fragments formed in interaction of ions ${}^3\text{He}^{2+}$ with isolated DKP molecules, in single-electron {211} and two-electron {202} trapping processes, obtained after the described processing procedure are shown in Figure 1.

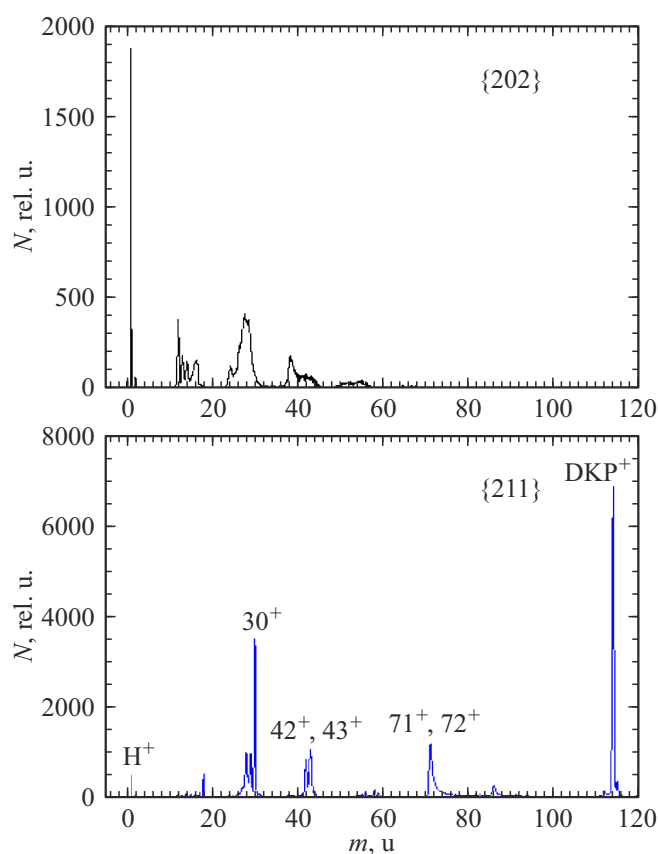


Figure 1. Mass spectra of fragments formed during single-electron {211} and two-electron {202} trapping processes in collision of ions He^{2+} with DKP molecules. Furnace temperature was 238°C .

Mass spectra of ions formed during {211} in interaction of ion He^{2+} with molecular jet formed during DKP heating contain a main intensity peak with mass $m = 114$ u. Analysis of obtained mass spectra allows to conclude that the molecular jet composition was not changed in temperature range $T = 170\text{--}276^\circ\text{C}$.

2. Quantum chemical calculations

To calculate optimized geometry of molecules and single-charged ions and their full energy, DFT method was used with Dmol³ module from Materials Studio software package. For calculations, B3LYP functionality and DNP all-electron atom basis (version 3.5) with unlimited spin polarization were selected [15,16]. The selected procedure provided repeatability by energy lower than 10^{-5} Hartree and geometrical — $5 \cdot 10^{-4}$ nm.

At the first stage, molecule and ion geometry optimization was performed by molecular mechanics method using COMPASS II, power field to minimize interatom interaction. At the second stage, DFT calculation of electronic structure with full geometry optimization was carried out. Calculated full molecule and ion energies were used for

Table 1. Relative cross-sections of elementary processes $\{2(2-s)n\}$ Relative number of protons formed during $\{2(2-s)n\}$ from the total number of recorded protons

| Process | σ , rel.u. | $N_{s,n}(\text{H}^+)/\Sigma_{s,n}N_{s,n}(\text{H}^+)$, % |
|-------------------|-------------------|---|
| $\Sigma_n\{21n\}$ | 50.0 ± 4.5 | 10.7 ± 0.7 |
| {211} | 45.3 ± 4.5 | 5.6 ± 0.6 |
| {212} | 4.3 ± 0.5 | 2.8 ± 0.3 |
| {213} | 0.4 ± 0.1 | 2.4 ± 0.3 |
| $\Sigma_n\{20n\}$ | 50.0 ± 4.4 | 89.3 ± 5.7 |
| {202} | 41.9 ± 4.3 | 38.3 ± 4 |
| {203} | 7.5 ± 0.7 | 41.4 ± 4 |
| {204} | 0.6 ± 0.2 | 9.7 ± 1 |

further analysis. Full energy data allow to calculate reaction energies for ion fermentation channels:

$$\Delta E_{re} = \Sigma E_{product} - \Sigma E_{reactant},$$

ΔE_{re} — reaction energy, $\Sigma E_{product}$ — sum of full energies of reaction products, $\Sigma E_{reactant}$ — sum of full energies of reacting particles, $\Delta E_{re} < 0$ — exothermic reaction, $\Delta E_{re} > 0$ — endothermic reaction.

3. Experimental results and discussion

3.1. Relative cross-sections of processes $\{2(2-s)n\}$

Relative cross-sections of change in charge state of collision partners are listed in Table 1. According to the listed data, during interaction between He^{2+} ion and DKP molecules the main single-electron trapping process by cross-section {211} efficiently flowing at high impact parameters $\sim 3-10$ au [17]. However, the sum of cross-sections of multielectron processes exceeds the process cross-section {211}.

It should be noted that formation of free protons as a result of interaction between DKP molecules and ion is caused mainly by multielectron processes, i.e. takes place during fragmentation of formed molecular ions $\{\text{DKP}\}^{n+}$ $n \geq 2$ (Table 1). Generally multielectron processes are efficiently carried out at lower impact parameters than that of the single-electron trapping process [18]. This fact shall be considered when addressing interaction of energy ions keV with condensed media where no collisions with high impact parameters occur.

3.2. Relative fragmentation cross-sections of single-charge ions DKP^+

Table 2 shows the main ion fragments formed during single-electron trapping in interaction between He^{2+} ions

and DKP molecules. Fragments shown in the table constitute 93% of the observed spectrum. Single-charged molecular ions DKP^+ formed during process {211} fragment with high probability, and mass spectrum of ion fragments formed during single-electron trapping has much in common with mass spectrum of fragments formed by electron impact [4]. Some difference in intensity of the ion fragments formed in these processes is explained by the fact that excitation of molecular ion DKP^+ depends on the structure of terms of the quasi molecular system formed in collision with ions $\{\text{HeDKP}\}^{2+}$ (e.g., [14]).

Identification of ion fragments was based on the assumption that formation of compounds with mass m requires minimum number of broken bond and minimum regrouping

Table 2. Relative intensity of ion fragments formed in the single-electron trapping process {211} in collision of He^{2+} ions with DKP molecules and in ionization of DKP molecules by electrons [3]

| m , u | Ion fragment | σ , rel.u. | σ , rel.u. [3] |
|---------|--|-------------------|-----------------------|
| 1 | H^+ | 16.1 | |
| 2 | H_2^+ | 0.4 | |
| 27 | HCN^+ , C_2H_3^+ | 13.2 | 6.6 |
| 28 | HCNH^+ , CO^+ | 49.2 | 55.1 |
| 29 | NH_2CH^+ | 43.0 | 32.7 |
| 30 | NH_2CH_2^+ , CH_2O^+ | 100.0 | 100.0 |
| 42 | $\text{C}_2\text{H}_2\text{O}^+$ | 28.6 | 31.6 |
| 43 | CHNO^+ | 42.9 | 27.7 |
| 44 | CH_2NO^+ | 7.4 | 3.0 |
| 56 | $\text{C}_2\text{H}_2\text{NO}^+$ | 3.7 | 5.7 |
| 57 | $\text{C}_2\text{H}_3\text{NO}^+$ | 2.0 | |
| 58 | $\text{C}_2\text{H}_4\text{NO}^+$ | 4.4 | 4.5 |
| 59 | $\text{C}_2\text{H}_5\text{NO}^+$ | 3.4 | |
| 71 | $\text{C}_3\text{H}_5\text{NO}^+$, $\text{C}_2\text{H}_3\text{N}_2\text{O}^+$ | 37.9 | 42.0 |
| 72 | $\text{C}_2\text{H}_4\text{N}_2\text{O}^+$ | 20.0 | |
| 73 | $\text{C}_2\text{H}_5\text{N}_2\text{O}^+$ | 8.8 | |
| 82 | C_3NO_2^+ , $\text{C}_4\text{H}_4\text{NO}^+$ | 2.1 | |
| 83 | C_3HNO_2^+ , $\text{C}_4\text{H}_5\text{NO}^+$ | 1.9 | |
| 86 | $\text{C}_3\text{H}_6\text{N}_2\text{O}^+$, $\text{C}_3\text{H}_4\text{NO}_2^+$ | 8.1 | 6.6 |
| 87 | $\text{C}_3\text{H}_5\text{NO}_2^+$ | 4.0 | |
| 112 | $(\text{M}-\text{H}_2)^+$ | 3.8 | |
| 113 | $(\text{M}-\text{H})^+$ | 3.8 | |
| 114 | $\text{C}_4\text{H}_6\text{N}_2\text{O}_2^+$ | 132.9 | 100.9 |
| 115 | $^{13}\text{CC}_3\text{H}_6\text{N}_2\text{O}_2^+$ | 8.1 | 5.7 |

Note. Data is rated to peak intensity with mass 30 u.

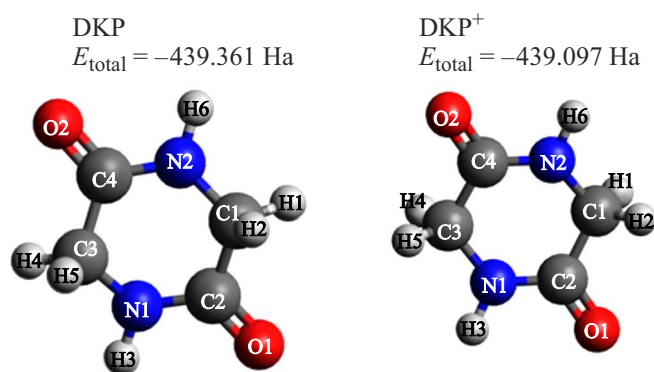


Figure 2. Structural formula of molecule (*M*) and ion (*I*) DKP with optimized geometry.

Table 3. Bond lengths in molecule (*M*) and ion (*I*) DKP with optimized geometry

| Bond | <i>R</i> , Å (<i>M</i>) | <i>R</i> , Å (<i>I</i>) | ΔR , Å (<i>I</i> – <i>M</i>) |
|-------|---------------------------|---------------------------|--|
| C2–C1 | 1.51138 | 1.51244 | 0.00106 |
| O1–C2 | 1.23652 | 1.22968 | –0.00684 |
| N1–C2 | 1.36534 | 1.35509 | –0.01025 |
| N1–C3 | 1.45209 | 1.44605 | –0.00604 |
| C4–C3 | 1.51217 | 1.5127 | 0.00053 |
| N2–C4 | 1.36547 | 1.35558 | –0.00989 |
| N2–C1 | 1.45125 | 1.44604 | –0.00521 |
| O2–C4 | 1.23666 | 1.22962 | –0.00704 |
| C1–H1 | 1.09292 | 1.10038 | 0.00746 |
| C1–H2 | 1.10442 | 1.09371 | –0.01071 |
| C3–H4 | 1.09289 | 1.10031 | 0.00742 |
| C3–H5 | 1.10411 | 1.09368 | –0.01043 |
| N1–H3 | 1.01588 | 1.01864 | 0.00276 |
| N2–H6 | 1.01582 | 1.01863 | 0.00281 |

of atoms between the formed ion and neutral fragments. It should be noted that hydrogen atom migration processes are probable during fragmentation. In particular, this indicates that H^{2+} ion has formed during fragmentation of single-charged ions DKP^+ (Table 2). Analysis of possible fragmentation channels was performed on the basis of structural schemes of a molecule and molecular ion shown in Figure 2 and bond length parameters calculated for conformations with optimized geometry. As shown in Table 3, molecule ionization in this case does not lead to noticeable increases in bond lengths which, as our calculations show, are typical of linear peptides for bonds breakage of which occurs with the highest probability [19].

Native molecular ion DKP^+ with mass $m = 114$ u is the main in the mass spectrum in terms of size. Peak with mass $m = 115$ u is caused by isotope component and has intensity 8.1 rel.u., which corresponds to the calculated data 7.5 rel.u. (5.7 rel.u. with relative intensity DKP^+ 100 rel.u.) [20].

Among the fragmentation processes, a process leading to formation of a fragment with mass $m = 30$ u, which can be identified as $NH_2CH_2^+$ or CH_2O^+ , is the main process in terms of cross-section. Fragment $NH_2CH_2^+$ is formed by separation of bonds C2–N1 (C4–N2) and C3–C4 (C2–C1) and hydrogen atom migration from neutral fragment to the formed ion (Figure 3). For reaction energy calculation, alternative processes were addressed namely abstraction of atom H6 (H3) (reaction 1a) and hydrogen atom bonded with carbon atom C1 (C3) (reaction 1b). When both reactions are addressed, radical with mass 84 was taken with optimized geometry shown in the figure. The listed data show that reaction 1a is more favourable in terms of energy. Calculations performed for a set of other isomers of radical with $m = 84$ u give a little higher reaction energies. Fragment $NH_2CH_2^+$ is formed by separation of bonds C4–N2 (C2–N1) and C4–C3 (C1–C2) and migration of two hydrogen atoms from neutral fragment to the formed ion (Figure 3 reaction 2). In terms of energy, formation of CH_2O^+ ion is less favourable than formation of $NH_2CH_2^+$ ion.

Formation of ion fragment $NHCH_2^+$ ($m = 29$ u, Figure 4) is caused only by separation of two bonds C2–N1 (C4–N2) and C3–C4 (C2–C1), however, as calculation shows, it is less favorable in terms of energy than the processes with hydrogen atom migration. One of the possible channels of the fragmentation process leading to formation of CO^+ ion with mass $m = 28$ u is also caused only by separation of bonds (Figure 5). According to the given data, this process has maximum energy among all described processes

Conclusion

The research included the analysis of molecular beam composition formed by formation of crystalline DKP. It was shown that molecular jet contains DKP molecules and does not change the composition in the temperature range $T = 170$ – $276^\circ C$. The measurements of relative cross-sections of change of charge state of collision partners has shown that the cross-section of two-electron trapping of cyclic DKP molecule is almost equal to the cross-section of single-electron trapping, and formation of free proton occurs in multielectron processes with formation of intermediate molecular ions DKP^{n+} $n \geq 2$. The study of fragmentation of molecular ions DKP^+ formed during single-electron trapping has shown their high resistance to fragmentation. Quantum chemical calculation of DKP geometry have shown that ionization process does not cause significant change in bond lengths. Reaction energy

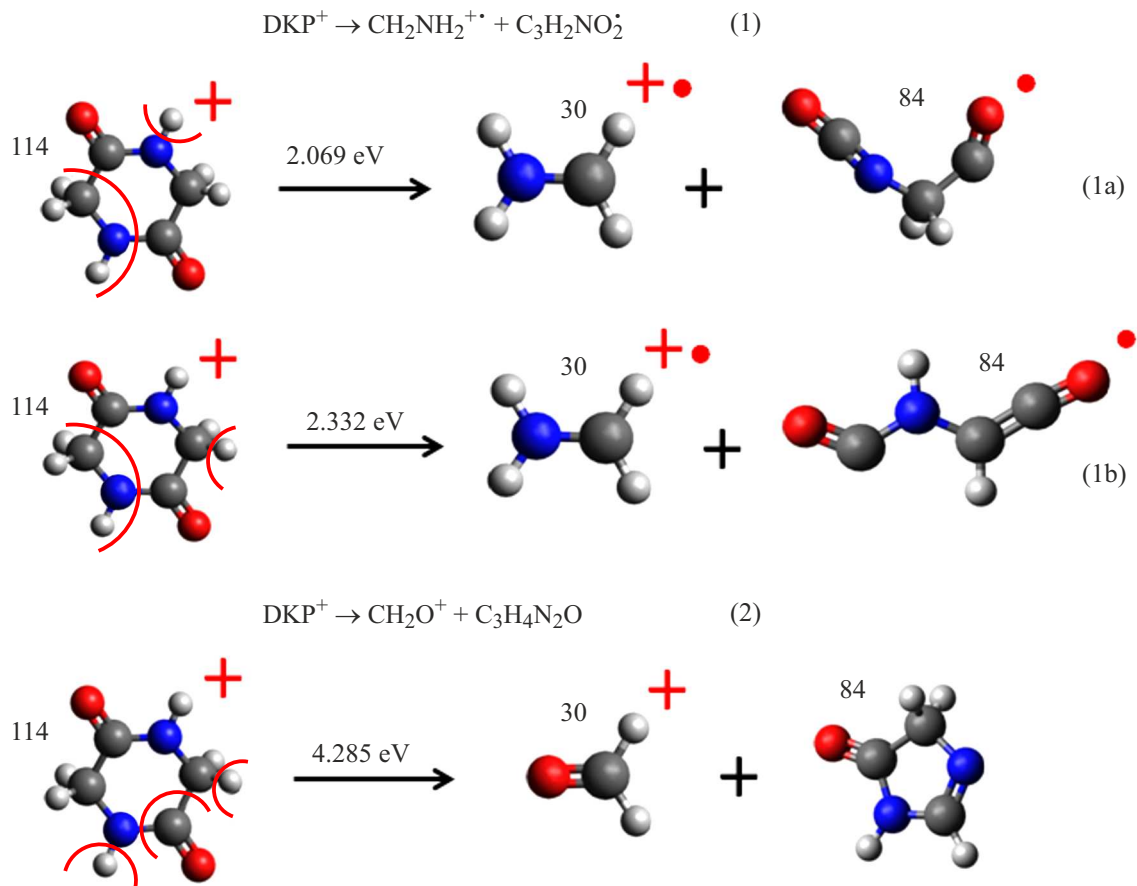


Figure 3. Fragmentation reactions causing fragment formation with $m = 30$ u.

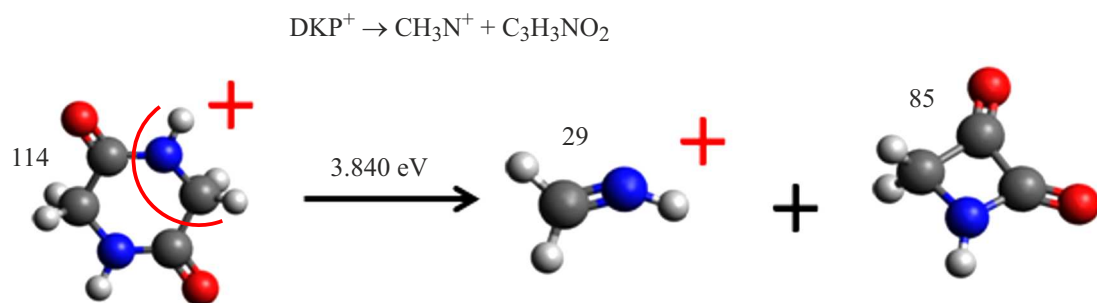


Figure 4. Fragmentation reaction causing fragment formation with $m = 29$ u.

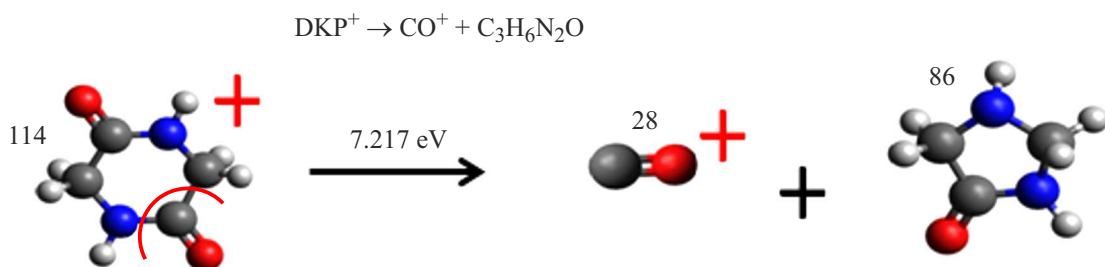


Figure 5. Fragmentation reaction causing fragment formation with $m = 28$ u.

calculations has shown that the most favourable in terms of energy are reactions followed by hydrogen atom migration.

Acknowledgments

Calculations were performed using the computational resources of the Resource Center Computational Center of the Saint Petersburg State University (<http://cc.spbu.ru>).

Funding

The work has been performed under the state assignment topic № 0040-2019-0023.

Conflict of interest

The authors declare that they have no conflict of interest.

References

- [1] Yu.B. Kudryashov. *Reaktsionnaya biofizika (ioiziruyushchie izlucheniya)* (Fizmatlit, M., 2004)
- [2] M.S. de Vries, P. Hobza. *Annu. Rev. Phys. Chem.*, **58**, 585 (2007). DOI: 10.1146/annurev.physchem.57.032905.104722
- [3] NIST Mass Spectrometry Data Center, W. E. Wallace, director, „Mass Spectra“ in NIST Chemistry Web-Book, NIST Standard Reference Database Number 69, Eds. P.J. Linstrom and W.G. Mallard, National Institute of Standards and Technology, Gaithersburg MD, 20899. <https://doi.org/10.18434/T4D303>
- [4] H.J. Svek, G.A. Junk. *J. Am. Chem. Soc.*, **86**, 2278 (1964).
- [5] V. Feyer, O. Plekan, R. Richter, M. Coreno, K.C. Prince, V. Carravetta. *J. Phys. Chem. A*, **113**, 10726 (2009). DOI: 10.1021/jp906843j
- [6] A.P. Wickrama Arachchilage, F. Wang, V. Feyer, O. Plekan, K.C. Prince. *J. Chem. Phys.*, **133**, 174319 (2010). DOI: 10.1063/1.3499740
- [7] A.P. Wickrama Arachchilage, F. Wang, V. Feyer, O. Plekan, K.C. Prince. *J. Chem. Phys.*, **136**, 124301 (2012). DOI: 10.1063/1.3693763
- [8] Y. Zhu, M. Tang, X. Shi, Y. Zhao. *Int. J. Quant. Chem.*, **107**, 745 (2007). <https://doi.org/10.1002/qua.20985>
- [9] A.P. Mendham, T.J. Dines, M.J. Snowden, B.Z. Chowdhry, R. Withnall. *J. Raman Spectrosc.*, **40**, 1478 (2009). DOI: 10.1002/jrs.2293
- [10] S. Celik, A.E. Ozel, S. Akyuz. *Vibr. Spectr.*, **83**, 57 (2016). <http://dx.doi.org/10.1016/j.vibspec.2016.01.007>
- [11] C.G. de Kruif, J. Voogd, J.C.A. Offringa. *J. Chem. Therm.*, **11**, 651 (1979).
- [12] D. Gross, G. Grodsky. *J. Am. Chem. Soc.*, **77**, 1678 (1955).
- [13] O.V. Smirnov, A.A. BasalaeV, V.M. Boitsov, S.Yu. Vyaz'min, A.L. Orbeli, M.V. Dubina. *Tech. Phys.*, **59**, 1698 (2014). DOI: 10.1134/S1063784214110231
- [14] V.V. Afrosimov, A.A. BasalaeV, O.S. Vasyutinskii, M.N. Panov, O.V. Smirnov. *Eur. Phys. J.D.*, **69**, 3 (2015). DOI: 10.1140/epjd/e2014-50435-5
- [15] B. Delley. *J. Chem. Phys.*, **92**, 508 (1990). <https://doi.org/10.1063/1.458452>
- [16] B. Delley. *J. Chem. Phys.*, **113**, 7756 (2000). <https://doi.org/10.1063/1.1316015>
- [17] R.K. Janev, L.P. Presnyakov. *Phys. Rep. (Rev. Sec. Phys. Lett.)*, **70**, 1 (1981).
- [18] V.V. Afrosimov, A.A. BasalaeV, K.V. Kashnikov, M.N. Panov. *FTT* **44** (3), 486 (2002). (in Russian).
- [19] A.A. BasalaeV, A.G. Buzykin, V.V. Kuzmichev, M.N. Panov, A.V. Petrov, O.V. Smirnov. *Pis'ma v ZhTF*, **47** (12), 23 (2021) (in Russian). DOI: 10.21883/PJTF.2021.12.51062.18746
- [20] Mass Spectrum Interpreter Version 2 Electronic source. Available at: <https://chemdata.nist.gov/mass-spc/interpreter/>